(NASA-CR-197110)
PROPULSION/AIRFRAME INTERFERENCE
FOR DUCTED PROPFAN ENGINES WITH
GROUND EFFECT Final Report, Mar.
1993 - Feb. 1995 (Mississippi
State Univ.) 17 p

N95-14909

Unclas

G3/05 0030494

Propulsion/Airframe Interference for Ducted Propfan Engines with Ground Effect

Abdollah Arabshahi and Ramesh Pankajakshan
Computational Fluid Dynamics Laboratory
Mississippi State University

The advanced propfan propulsion systems design of the next–generation subsonic transport aircraft has been of interest to many airline companies in the past several years. This is due to the studies which indicate that an efficient ducted propfan engine technology offers a significant reduction in aircraft fuel consumption. However, because of the geometric complexity of the configuration, one challenge is the integration of the ducted propfan engine with the airframe so that aerodynamic interference effects frequently encountered near the nacelle can be minimized, or perhaps, optimized. To understand this interaction phenomenon better, it is desirable to have a reliable and efficient computational tool that can predict propeller effects on the flowfield around complex configurations.

The concern of an airplane designer is not focused on the detail analysis of the flow through or about the propulsion system (blade–to–blade flowfield), but rather on the interference effects generated by the propulsion system and the airframe; however, the propulsion system must be adequately simulated. To this end, an approach has been developed that simulates the aircraft propulsive devices by the use of body force terms in the Euler and/or Navier–Stokes equations. This approach provides for the natural interaction between the propulsion system and the airframe because the interaction is determined from the simultaneous solution to the complete system of equations and not from some ad hoc pre or post processing operation. This technique is not new. It has been successfully employed to compute flowfield around complicated three–dimensional propfan configuration by Whitfield and Jameson [Ref.1]. Pankajakshan et al. [Ref. 2] used the body force approach for the development of numerical alogrithms which can accurately simulate the inviscid flowfield through three–dimensional ducted propfan configurations. However, the eventual goal of this project is to develop a practical general purpose Navier–Stokes flow solver which accurately models the three–dimensional fluid flow about wing/engine/body configurations. In an effort toward this goal, the existing inviscid multiblock flow solver is extended to solve the three–dimensional, conservation–law form of the Reynolds–averaged Navier–stokes equations with thin–layer approximation. Turbulence is modeled using the well known Baldwin and Lomax [Ref. 3] mixing length model.

In order to demonstrate the performance and applicability of the present flow solver, the computations were performed for subsonic viscous flow about the Pratt Advanced Ducted Propfan within close proximity of a ground plane at three different flight conditions. These test cases are: (1)

static engine simulation with static ground plane, (2) static engine simulation with moving ground plane, and (3) moving engine simulation with static ground plane.

The geometry employed in this study was the Pratt Advanced Ducted Propfan (Pratt ADP) with the long cowl in the vicinity of a ground plane. The geometry and the computational grid is shown in Figure 1. The computational region for the configuration is divided into four blocks containing a total of approximately 124,000 grid points. The maximum and minimum number of grid points in a block are approximately 69,000 and 15,000, respectively. A side view of Pratt ADP engine is presented in Figure 2, while Figure 3 shows a view looking downstream at a plane about mid–chord. As the Pratt ADP geometry is symmetric, only one–half of the configuration is modeled. The grid points are closely packed near the surfaces to resolve the boundary layers effectively. This case simulates the engine near the ground before take–off or after a landing situation with the outer cowl at a height of one–third the maximum engine radius above the ground.

The first study focuses on simulating the static Pratt ADP engine operating within close proximity of the static ground plane. The simulation was to observe whether the proximity of the ground had any significant effect on the engine flow field. The effects of the propfan are imparted to the flowfield using body force values calculated from the pressure jumps obtained from the experiment [4]. The magnitude of the total pressure ratio (total pressure jump across the propeller fan) employed in these calculations is 1.287. An adaptive approach [Ref. 2] has been used for achieving the desired force components at the propeller and the increase in the stagnation pressure across the propeller. A turbulent viscous solution has been obtained for this geometry for a freestream Mach number 0.30 at zero degree angle of attack and Reynolds number of 4.5 million based on the length of the spinner. Figure 4 demonstrates the computed surface pressure distribution on the outer cowl. Evidence of the noticeable variation in pressure caused by proximity to the ground plane is mostly pronounced in the mid–section region of the nacelle and will exert a relatively strong force pulling the engine toward the ground plane. In Figure 5 identical pressures are seen everywhere on the inner cowl except for a few points near X/L=0.3 and X/L=0.5 where there is slight variation. Figure 6 presents the distributions of the pressure coefficient on the ground plane. It is evident from Figure 6 that the pressure drop ahead of the engine inlet results from the flow acceleration by the simulator and builds up again at the exit. Presented in Figure 7–8 are the velocity and pressure distributions on the plane of symmetry respectively, while Figure 9 displays the overall surface pressure distribution of the spinner, nacelle, and ground plane. This was done to gain better understanding of the salient features of the flowfield structure and show the influence of the ground plane on the powered engine at a before take–off or after landing condition. As the velocity distribution in Figures 8 indicates, flow inside the nacelle is accelerated to a higher Mach number than freestream due to the divergent section and simulator of the nacelle. The boundary layer becomes thicker aft of this acceleration resulting in a recirculating flow region near X/L=0.3.

The second study focuses on simulating the static Pratt ADP engine operating within close proximity of a moving ground plane at the speed of freestream (i.e. M=0.30). The motivation for this study was to determine whether a moving ground had any significant effect on the engine flowfield compared with the previous study (static ground plane), and to circumvent some of the concerns with the experimental tests that were performed with a static or moving ground plane. This case was run at a freestream Mach number of 0.30 for zero degree angle of attack. The Reynolds number was 4.5 million based on the length of the spinner. Presented in Figures 10–13 are the numerical results for the flow past the static Pratt ADP engine operating near the moving ground plane. Figures 10–12 illustrates pressure distributions on the surfaces of both the nacelle (outer and inner surface) and the ground plane; while Figure 13 shows the overall surface pressure distribution of the spinner, nacelle, and ground plane. A comparison of the numerical results of this study (moving ground plane) with the previous numerical solutions (static ground plane) indicated a negligible change in the surface pressure distributions due to motion of the ground plane.

The third study focuses on simulating the dynamic Pratt ADP engine operating within close proximity of a static ground plane. The solution for this case was obtained by setting the ground plane and freestream velocity to zero and giving the entire grid about the engine a grid speed of the negative of the freestream velocity of the second study. A comparison of computed surface static pressure distributions of this case with the second case numerical solutions indicated that there is no noticeable difference in the surface static pressure distributions.

REFERENCES

1. Whitfield, D.L., and Jameson, A., "Euler Equation Simulation of Propeller–Wing Interaction in Transonic Flow," *Journal of Aircraft*, Vol. 21, No. 11, pp 835–839, November 1984.
2. Pankajakashan, R., Arabshahi, A., and Whitfield, D.L., "Turbofan Flowfield Simulation Using Euler Equations with Body Forces," AIAA Paper 93–1978, June 1993.
3. Baldwin, B.S., and Lomax, H., "Thin–Layer Approximation and Algebraic Model for Separated Turbulent Flows," AIAA–78–257, January 1978.
4. Hughes, C., Private Communications, NASA Lewis Research Center, 1993.

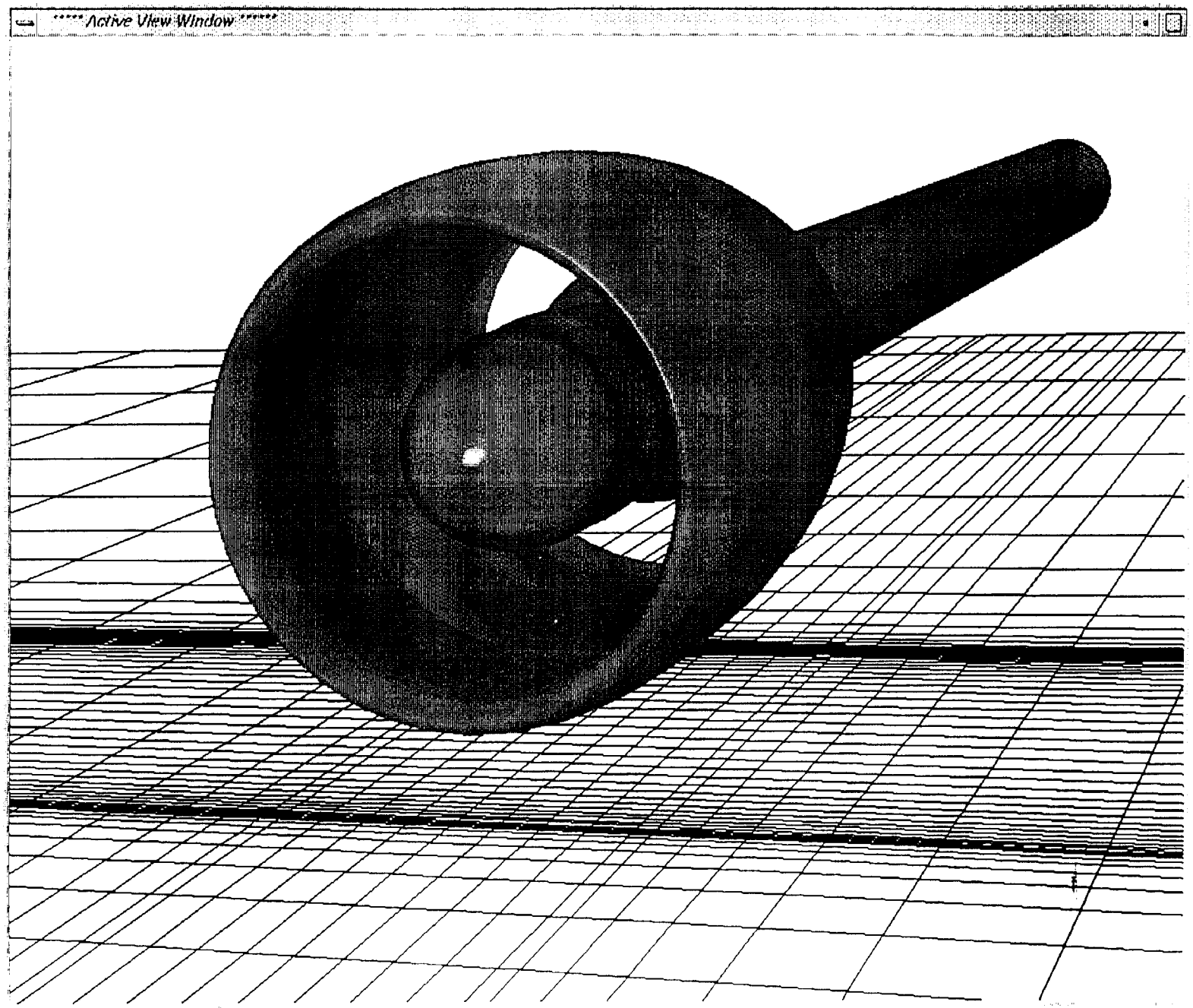

Figure 1. Pratt advanced ducted propfan (Pratt ADP) with ground plane

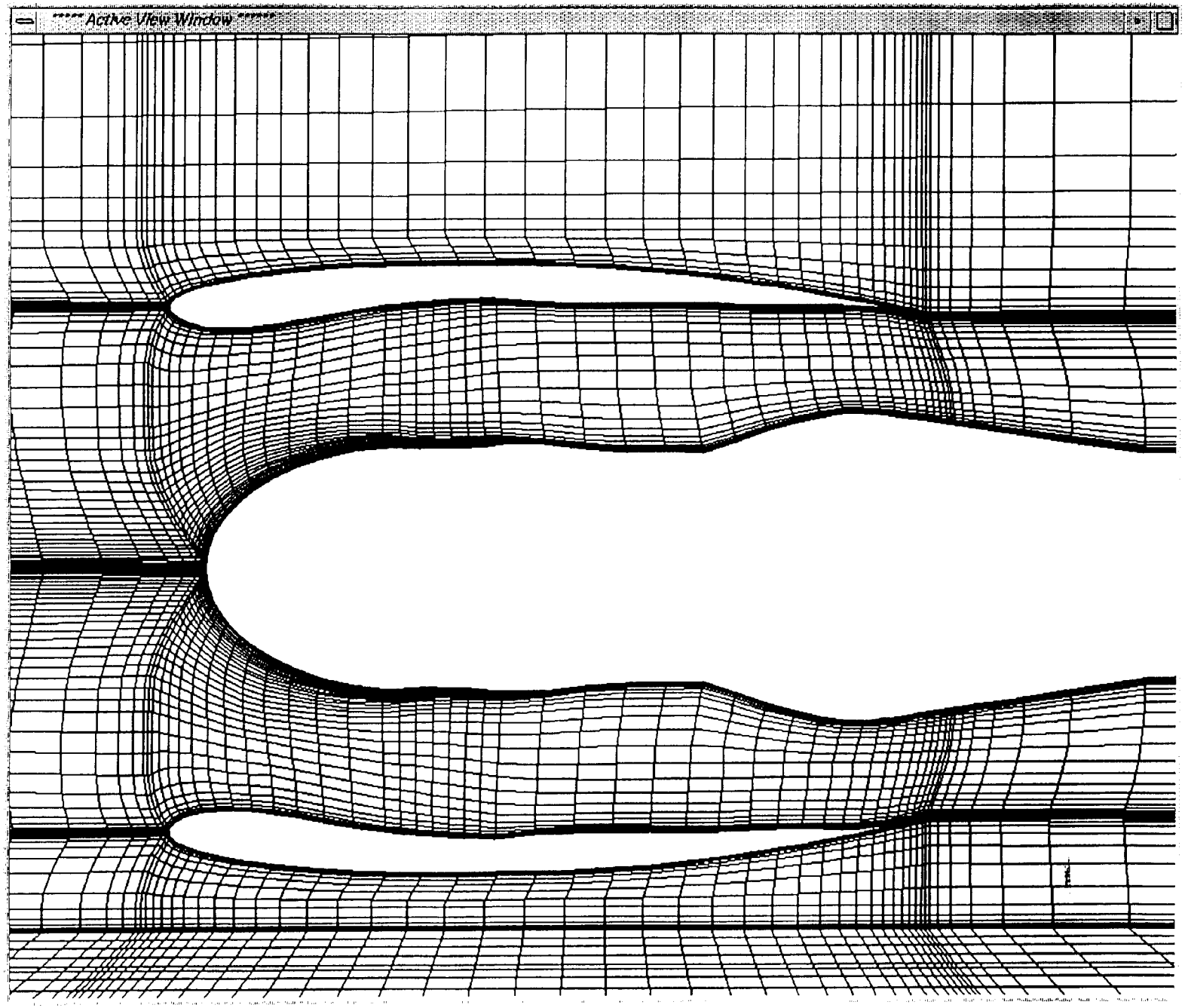

Figure 2. Side view of Pratt ADP configuration

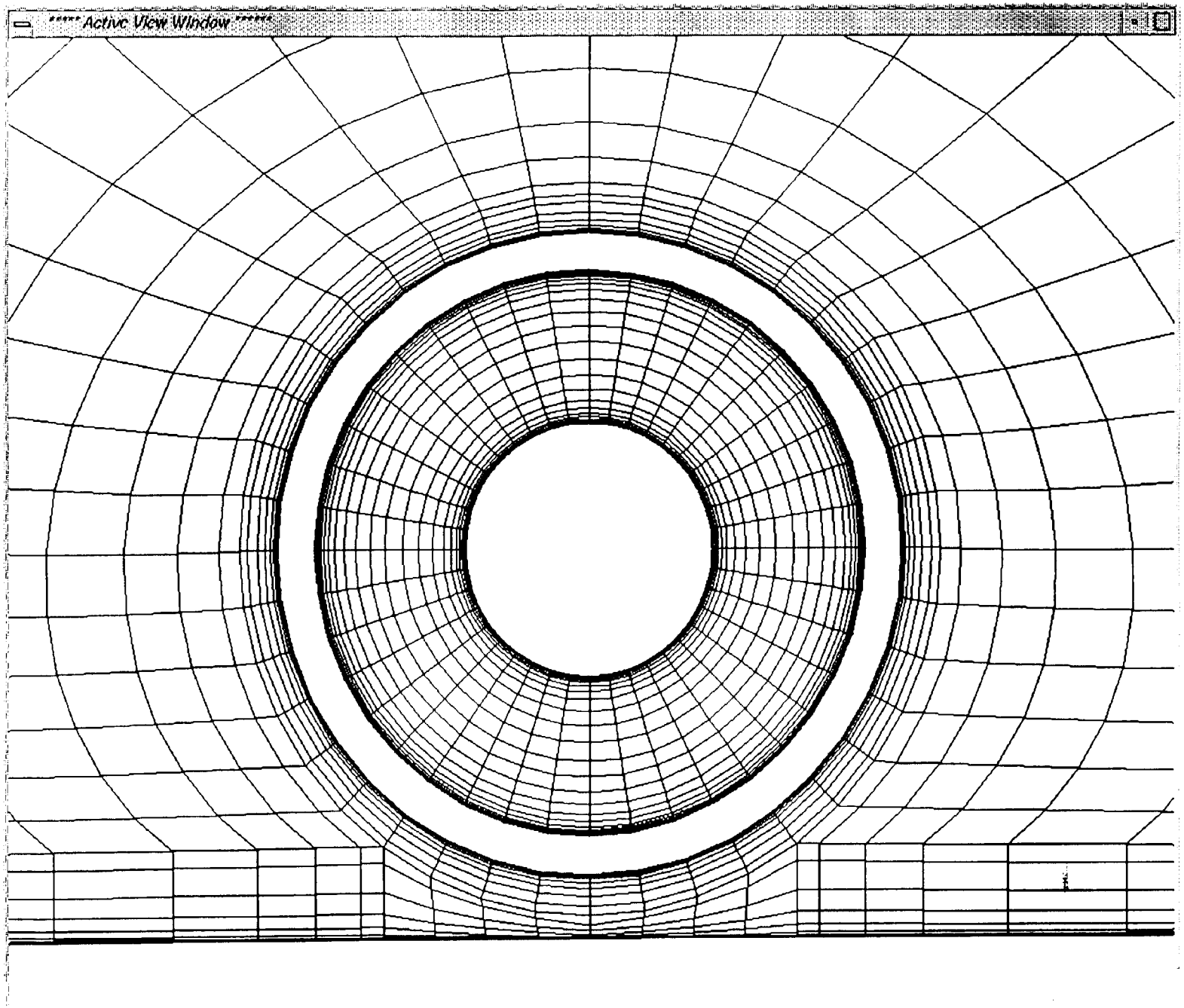

Figure 3. Front view of Pratt ADP configuration

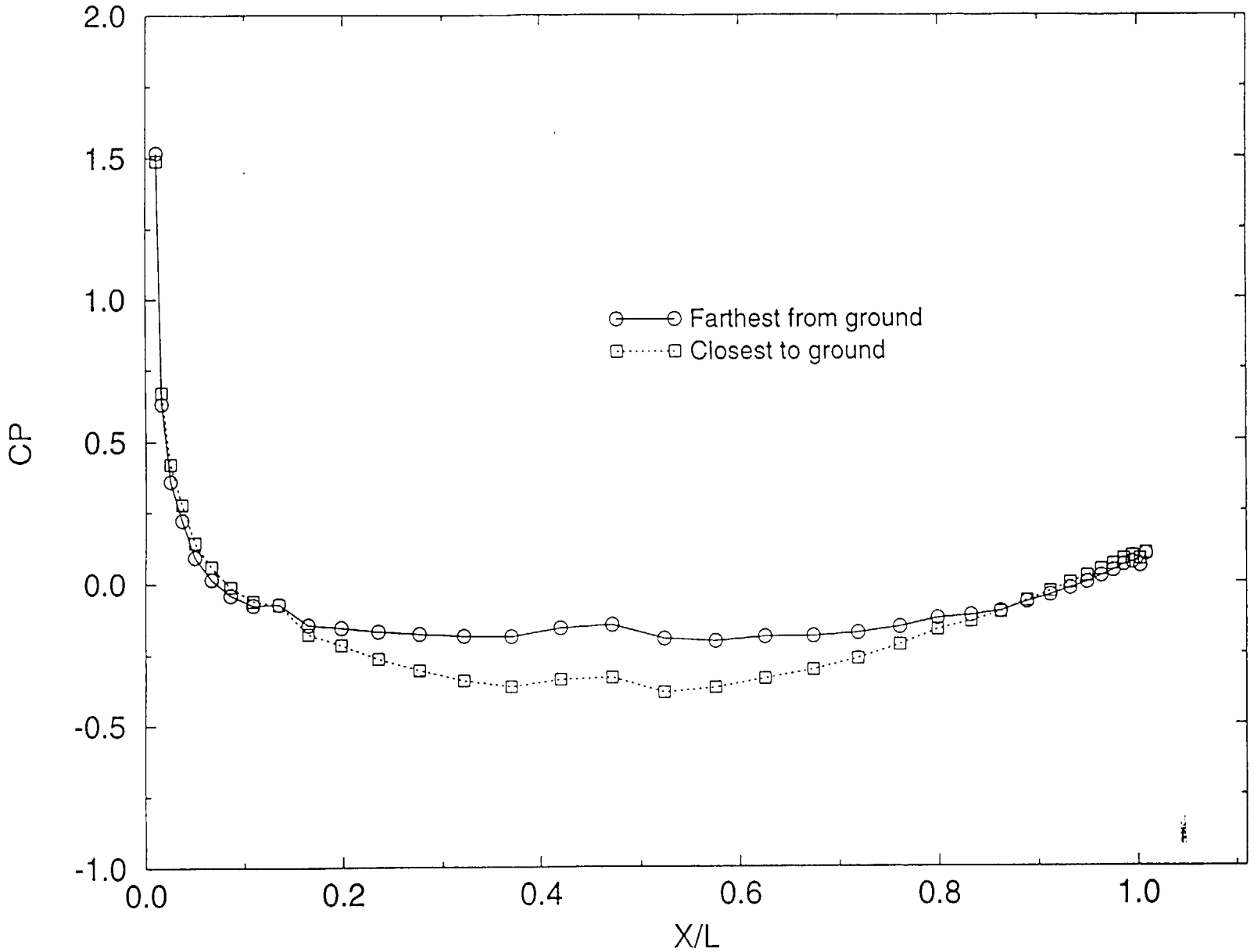

Figure 4. Pressure distribution on external surface of Pratt ADP with ground effect

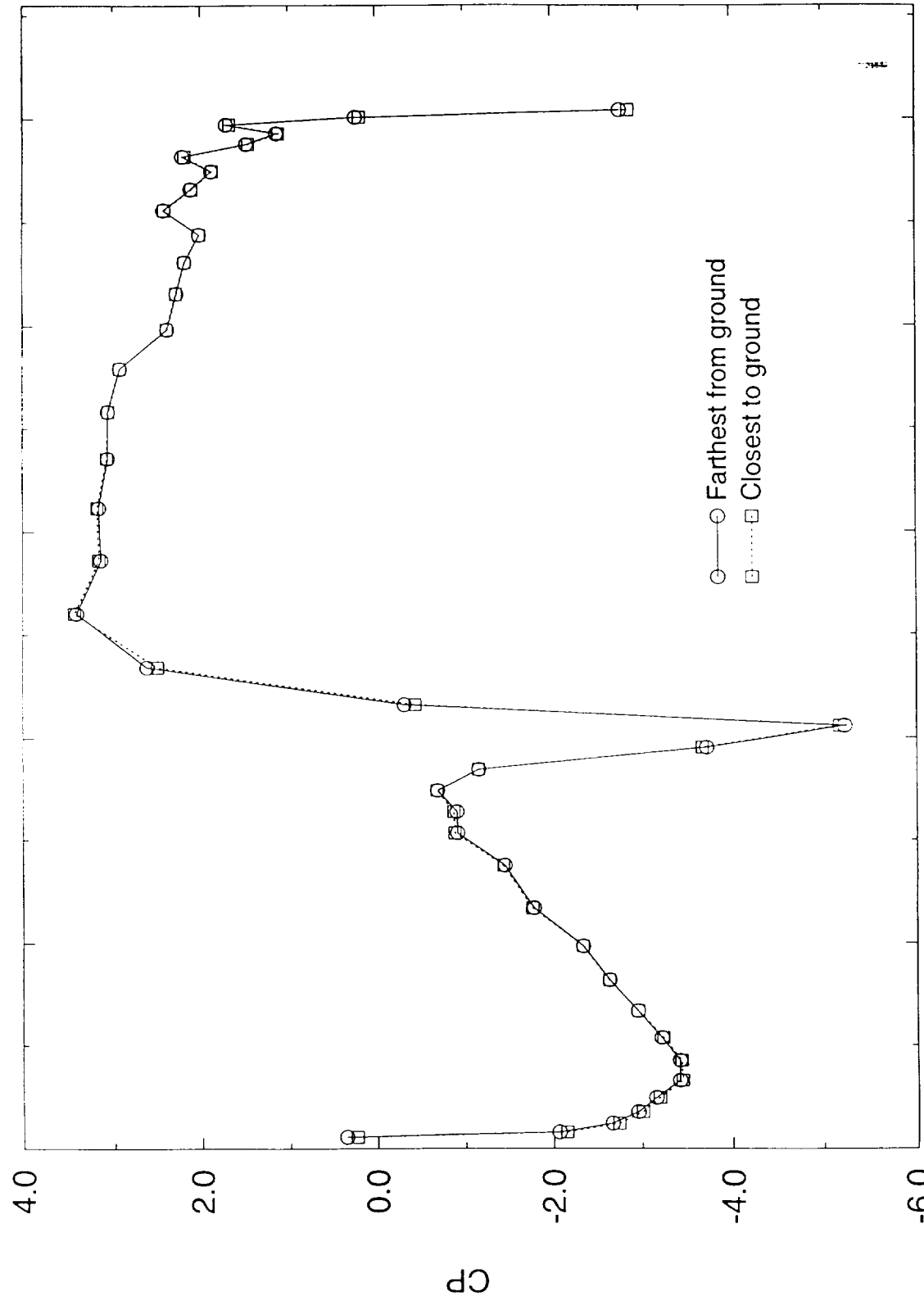

Figure 5. Pressure distribution on internal surface of Pratt ADP with ground effect

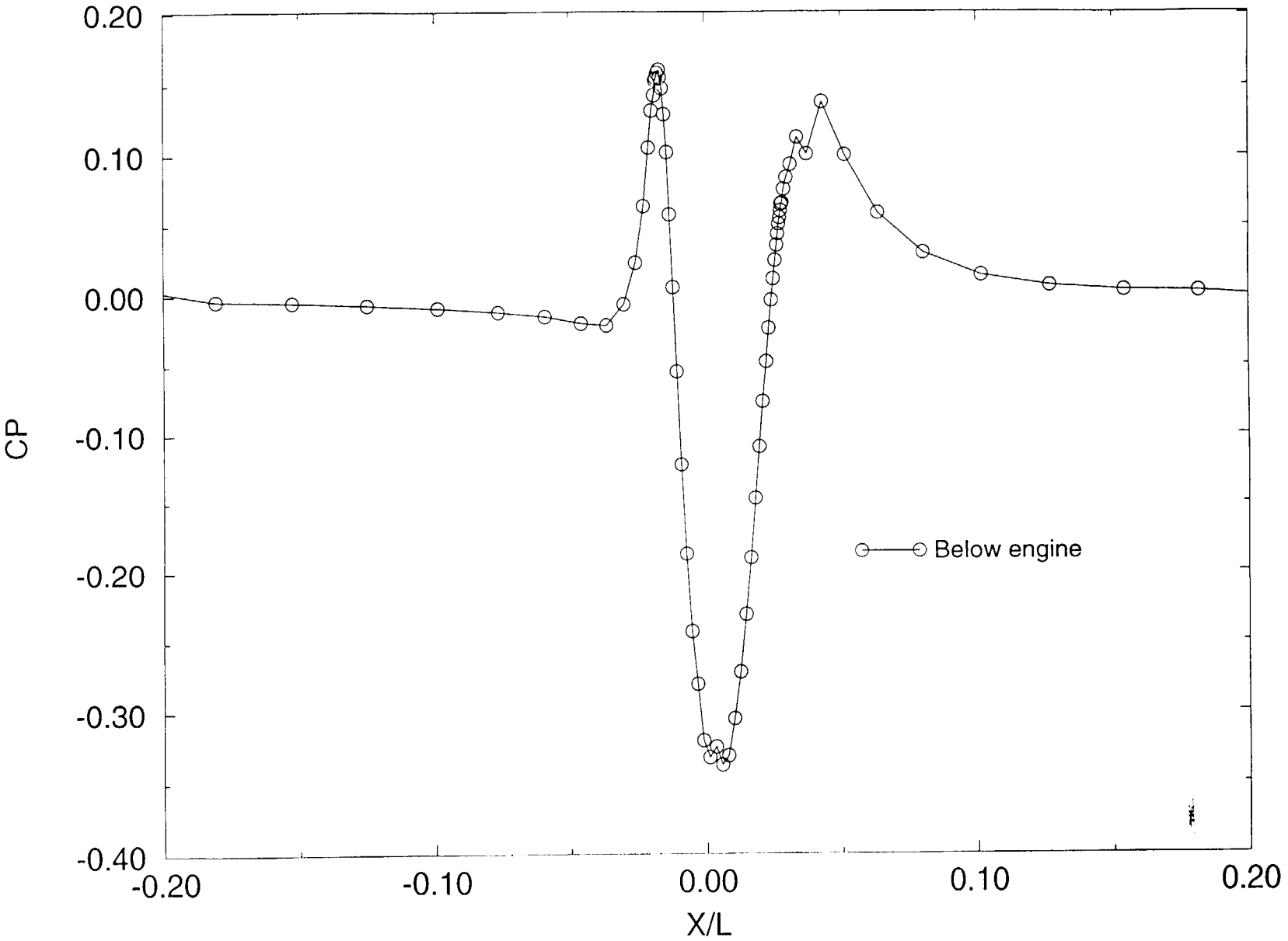

Figure 6. Pressure distribution over ground showing proximity effects of engine

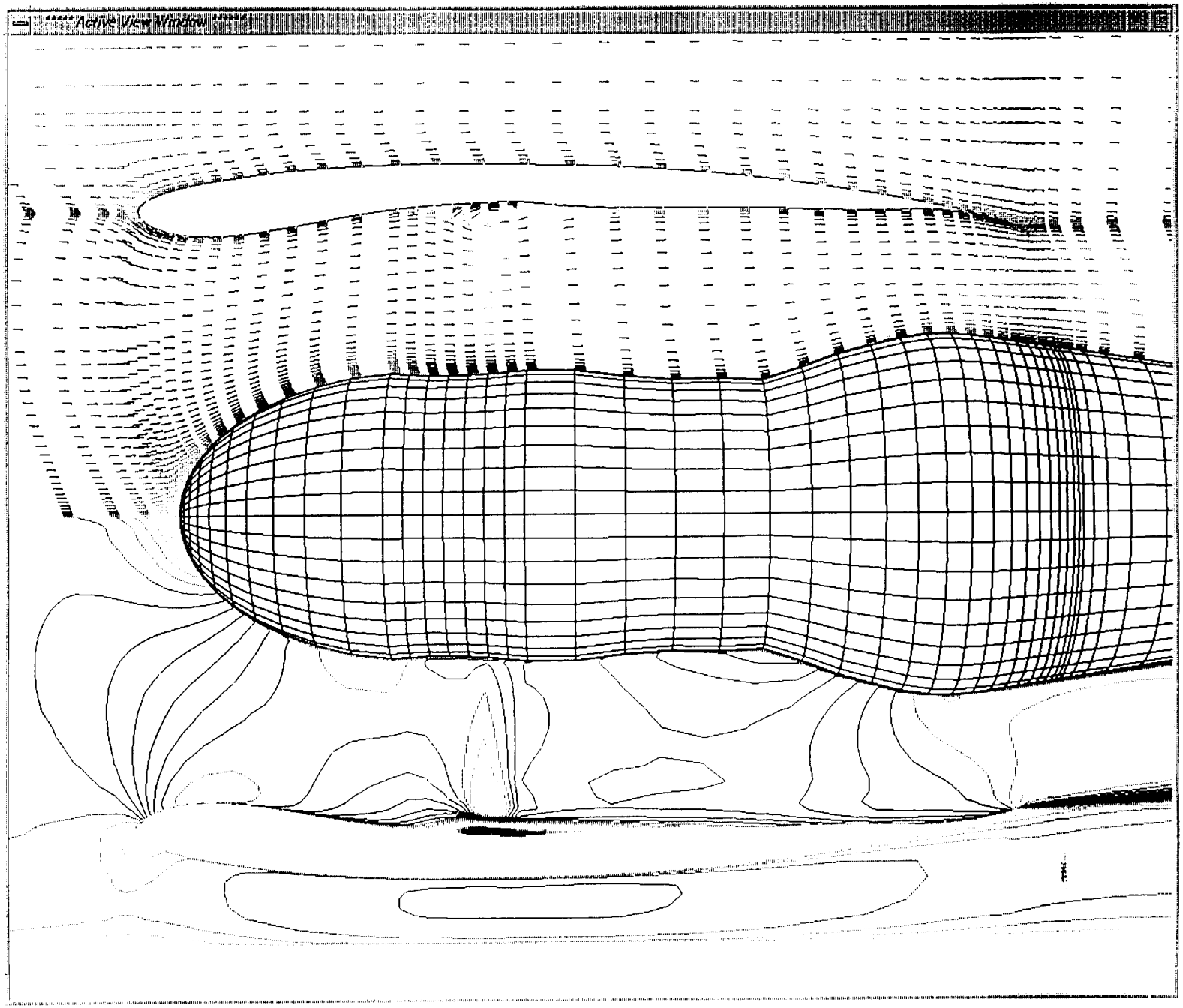

Figure 7. Computed velocity distribution

Figure 8. Computed pressure distribution

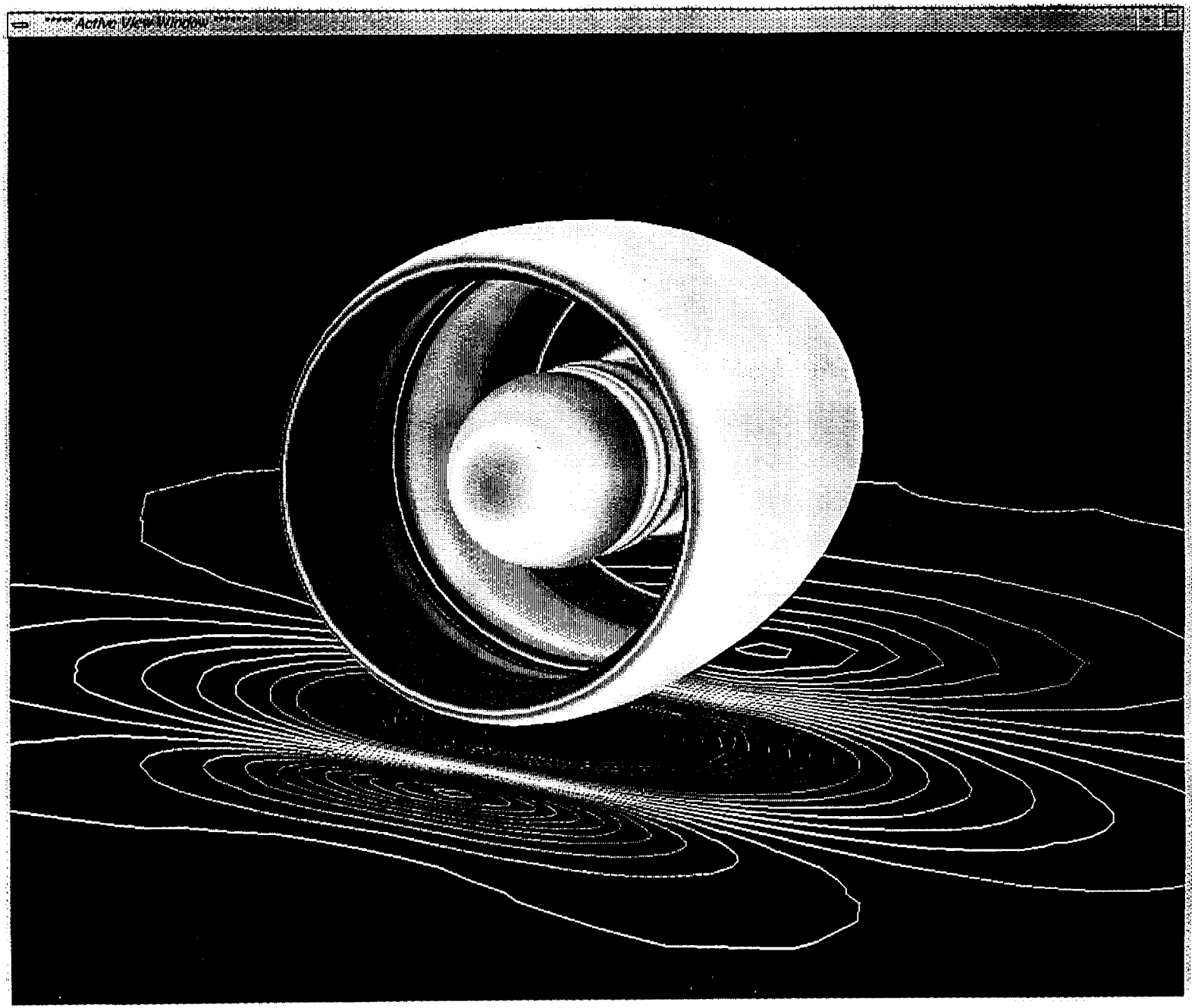

Figure 9. Computed surface pressure contours over Pratt ADP engine and static ground plane

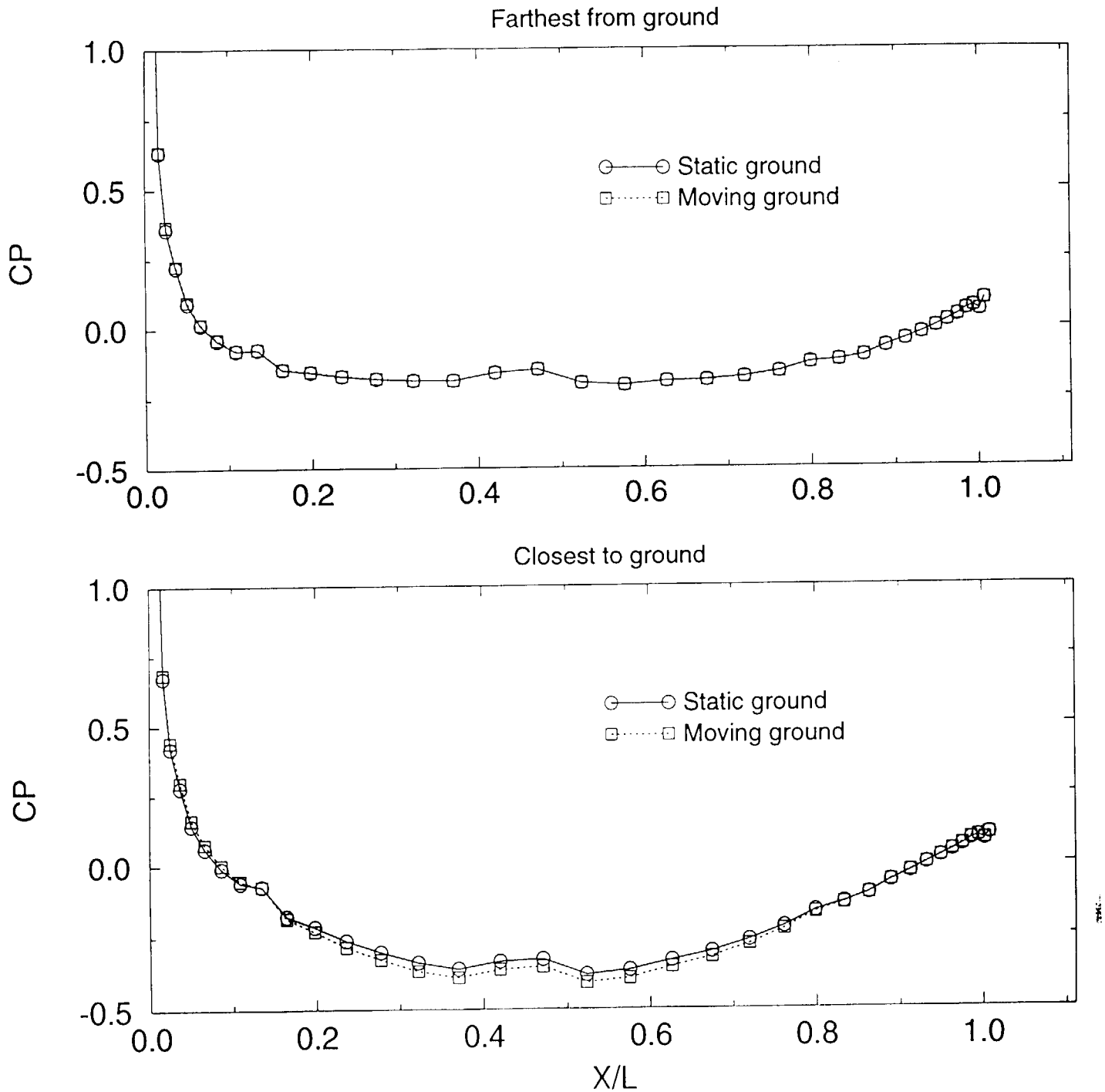

Figure 10. Pressure distribution on external surface of Pratt ADP engine within close proximity of a static and moving ground plane

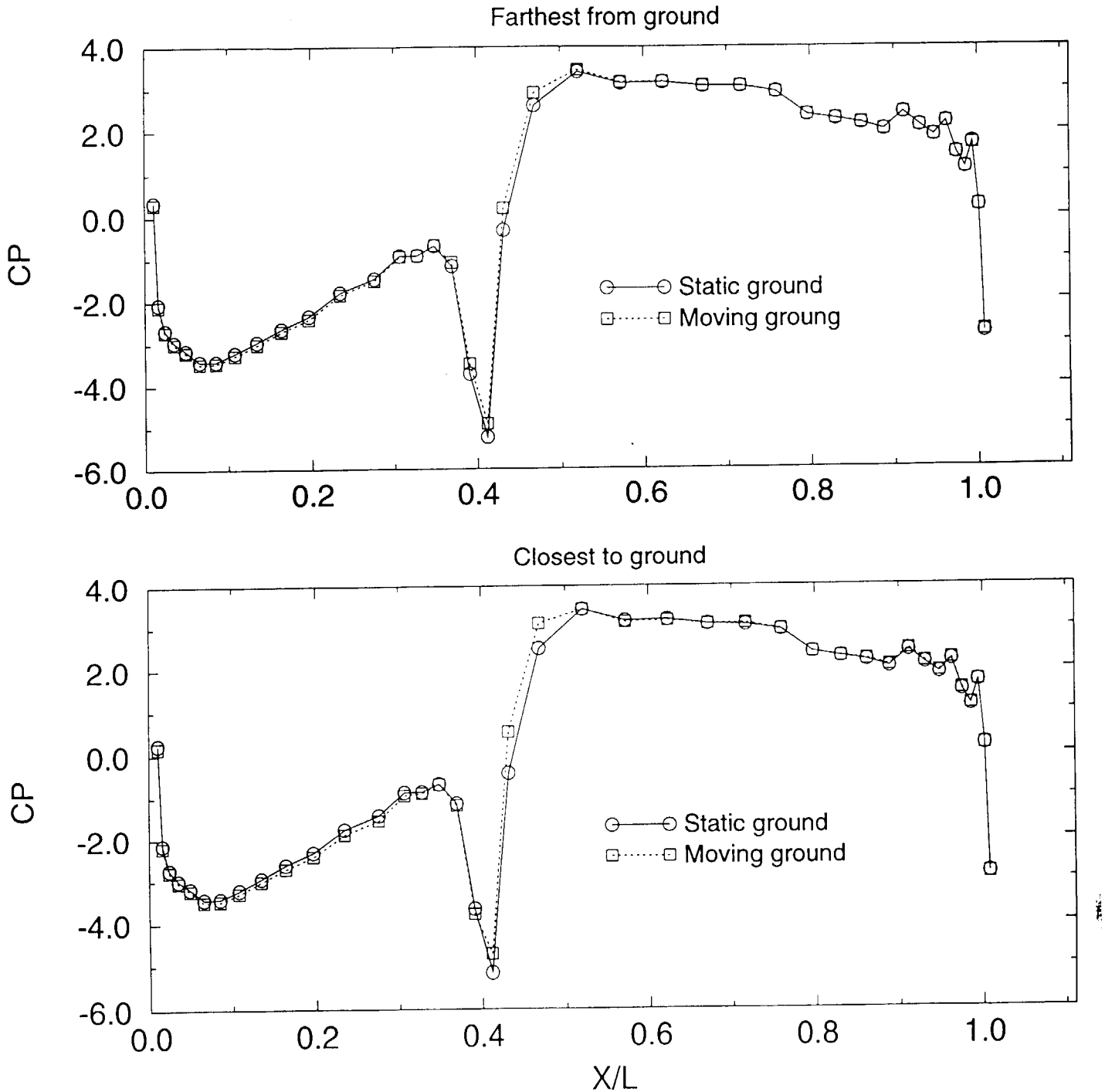

Figure 11. Pressure distribution on internal surface of Pratt ADP engine within close proximity of a static and moving ground plane

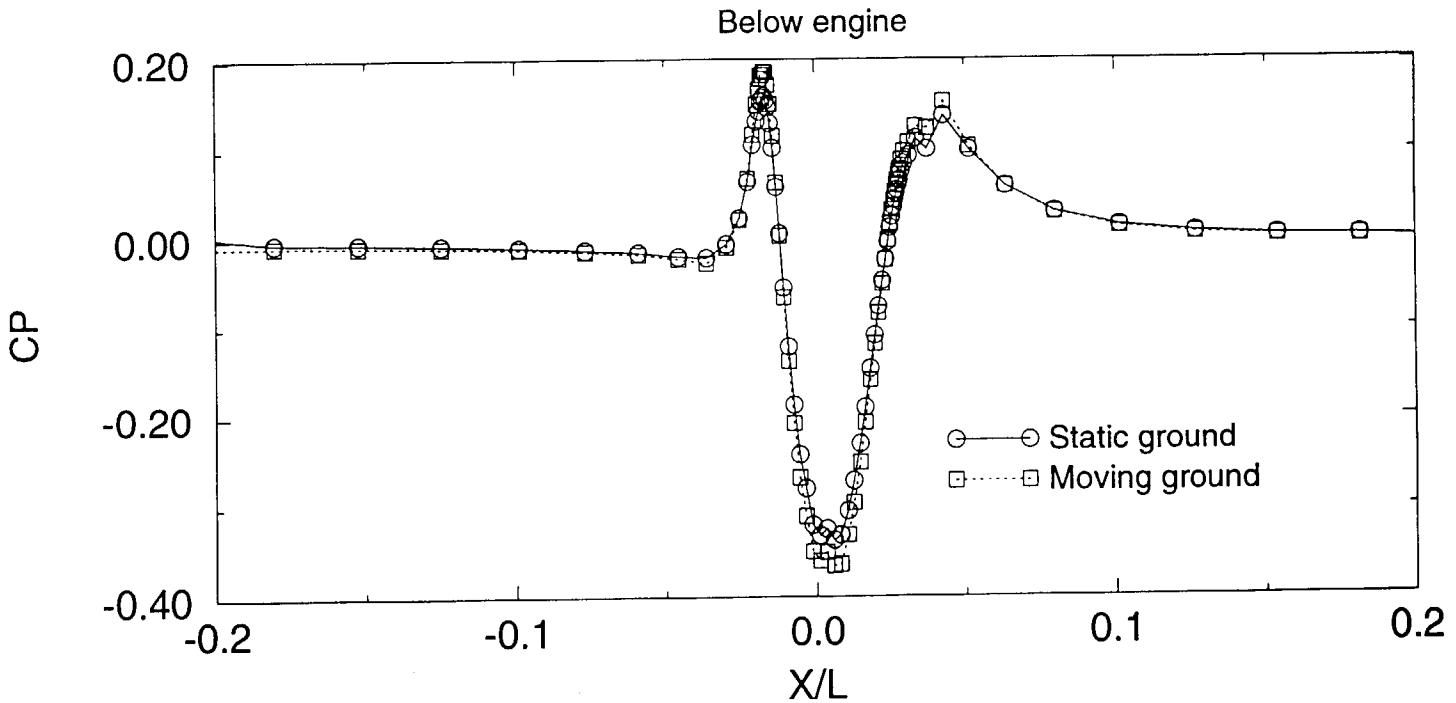

Figure 12. Pressure distribution over static and moving ground plane showing proximity effects of engine

Figure 13. Computed surface pressure contours over Pratt ADP engine and moving ground plane